Experimental Validation and Performance Measurements of an ECR Thruster Operating on Multiple Propellants

IEPC-2019-199

Presented at the 36th International Electric Propulsion Conference
University of Vienna • Vienna, Austria
September 15-20, 2019

R. Moloney[1], B. Karadag[2], and A. Lucca Fabris[3]
Surrey Space Centre, University of Surrey, GU2 7XH, Guildford, United Kingdom

D. Staab[4], A. Frey[5], A. Garbayo[6], L. Shadbolt[7], and E. Rosati Azevedo[8]
AVS UK Ltd, Rutherford Appleton Laboratory, OX11 0QX, Chilton, United Kingdom

and

D. Faircloth[9], S. Lawrie[10], and O. Tarvainen[11]
STFC ISIS Spallation Neutron and Muon Facility, Rutherford Appleton Laboratory, OX11 0QX, Chilton, United Kingdom

Abstract: The AQUAJET propulsion system is currently under investigation and development within Surrey Space Centre, at the University of Surrey, in a collaboration with AVS UK Ltd., STFC, and SSTL, to address the growing market need for low-cost, low-power propulsion for small communication satellites and constellations. The propulsion system is based on electron cyclotron resonance (ECR) heating using a microwave frequency of 2.45 GHz, and employing a single hollow cylindrical permanent magnet, to produce a magnetic nozzle and ambipolar acceleration. Due to its cathodeless design, the propulsion system is suitable for use with a wide range of alternative propellants, allowing the market to move away from high-cost and low-abundance xenon. The proof-of-concept thruster prototype has a flexible modular design allowing for testing of multiple geometric configurations. Experimental validation of the AQUAJET thruster has been successfully implemented with argon, xenon, and water. Direct thrust measurements have been obtained, using a pendulum-type thrust balance, while operating at load power levels between 17-171 W with multiple propellants at a range of mass flow rates. AQUAJET has demonstrated thrust, and specific impulse of up to: 0.72 mN, 736 s at 171 W (load power) with argon; 0.83 mN, 861 s at 143 W (load power) with xenon; and 0.26 mN, 188 s at 82 W (load power) with water.

[1] PhD Candidate in Space Engineering, r.moloney@surrey.ac.uk
[2] Research Fellow, Electric Propulsion Laboratory, b.karadag@surrey.ac.uk
[3] Head of Electric Propulsion Laboratory and Lecturer in Space Propulsion, a.luccafabris@surrey.ac.uk
[4] Electric Propulsion Engineer, dstaab@a-v-s.uk.com
[5] Space Project Manager, afrey@a-v-s.uk.com
[6] Business Development Manager and Senior Mechanical Engineer, agarbayo@a-v-s.uk.com
[7] Space Project Engineer, lshadbolt@a-v-s.uk.com
[8] Electric Propulsion Engineer, erosati@a-v-s.uk
[9] Low Energy Beam Group Leader, ISIS, dan.faircloth@stfc.ac.uk
[10] Ion Source Section Leader, ISIS, scott.lawrie@stfc.ac.uk
[11] Rutherford International Fellow, olli.tarvainen@stfc.ac.uk

Nomenclature

Ar	=	argon
AVS	=	Added Value Solutions
CRM	=	Collisional Radiative Model
ECR	=	Electron Cyclotron Resonance
EP	=	Electric Propulsion
GEO	=	Geosynchronous Earth Orbit
GIE	=	Gridded Ion Engine
H_2O	=	water
HET	=	Hall Effect Thruster
I_{sp}	=	specific impulse, s
LEO	=	Low Earth Orbit
$\dot{m}_p$	=	propellant gas mass flow rate, mg/s
η_T	=	thruster efficiency, %
OES	=	Optical Emission Spectroscopy
P	=	microwave power, W
P_{bg}	=	background pressure, mbar
QCT	=	Quad Confinement Thruster
SSC	=	Surrey Space Centre
SSTL	=	Surrey Satellite Technology Ltd.
STFC	=	Science & Technology Facilities Council
T	=	thrust, mN
TRL	=	Technology Readiness Level
T_e	=	electron temperature, eV
Xe	=	xenon

I.Introduction

THERE has been steady growth in the use of electric propulsion (EP) systems over the last few decades, such as Hall Effect Thrusters (HETs), and Gridded Ion Engines (GIEs), for satellite applications (particularly in communication satellites) for orbit insertion and station-keeping in Low Earth Orbit (LEO) and Geosynchronous Earth Orbit (GEO) missions[1,2]. It is anticipated that several thousand small satellites will be launched over the next 5-10 years, many of which will be deployed as constellations containing up to 1000's of spacecraft[3]. Many of these constellations are expected to employ some form of on-board propulsion. The propulsion requirements of these small satellites and constellations calls for small-scale, low-power EP devices, for which application HETs and GIEs are unsuitable. Although HETs and GIEs have accumulated significant flight heritage over the past 50+ years and have remained the top contenders for many space applications, a number of inherent problems restrict these established technologies from satisfying the requirements of the ever-growing small satellite industry. The efficiency of these systems is significantly reduced when scaling down to smaller size and lower power, as the increase in the ratio of discharge channel surface area to plasma volume results in greater losses to the thruster walls[4,5]. The complexity and cost of these systems is increased by the necessity for external neutralizers, which often employ thermionic insert materials susceptible to contamination, that impose restrictions on propellant choice to expensive, high purity noble gasses such as xenon. In addition, the need for external neutralizers and grids, and the increase in plasma losses when scaling down, result in reduced thruster lifetime due to erosion.

This gap in the market has led to a collaboration between SSC (at the University of Surrey), AVS UK Ltd., STFC, and SSTL, which is funded by the UK Space Agency, on the development and investigation of a new electrodeless, water-propelled Electron Cyclotron Resonance (ECR) thruster: AQUAJET. The AQUAJET thruster is a potentially scalable, cathodeless ambipolar plasma source utilizing ECR at 2.45 GHz with a simple permanent magnet configuration to provide thrust at low power. Its modular design provides a test-bed for multiple geometric thruster configurations, giving flexibility of thruster optimization for operation with different propellants. This new technology is designed as a low-cost solution to address the problems with lifetime limitations, scalability, and compatibility with unconventional propellants, that are prominent among the established technologies in use today.

The following sections provide a description of the AQUAJET thruster, and the experimental apparatus used to validate proof-of-concept, and evaluate thruster performance. An overview of the experimental validation and initial thruster performance measurements collected at SSC, while operating the thruster with multiple propellants are presented and discussed.

II.AQUAJET Thruster

The AQUAJET thruster has a modular design that allows for testing of multiple geometric configurations, including three chamber radii (8, 10, and 12 mm) and a variety of discharge chamber lengths (6, 8, 10, and 12 mm for the radius 8, and 10 mm chambers, and 8, 10, 12, and 14 mm for the radius 12 mm chamber), with an adjustable ECR zone position. A detailed description of the thruster design was published previously in Ref. 6. The main components of the thruster are shown in Fig. 1 a), and the thruster assembly is shown in Fig. 1 b). A microwave signal of 2.45 GHz is supplied to an axial copper antenna via a series of coaxial cables, and a DC block to isolate (in DC) the thruster from the generator obtaining a floating configuration. The antenna is supported by an aluminium baseplate and is located at the centre of a cylindrical aluminium discharge chamber; it is insulated from the plasma by a dielectric slab and sleeve made from boron nitride. Three brass inlets feed propellant directly into the discharge chamber via small holes in the chamber walls. A set of aluminium washers provide additional lengths to the discharge chamber and allow for the adjustment of the ECR zone position by increasing the distance between the magnet and the discharge chamber.

An annular samarium cobalt permanent magnet, with a remanence of 1.08 Tesla, is located behind the antenna, inside aluminium housing. The magnet is designed to produce an axial magnetic field profile that: (i) increases in strength towards the back wall of the chamber, (ii) reduces in strength towards the exit plane of the thruster, and (iii) diverges downstream of the exit plane, as illustrated in Fig. 2. This establishes a magnetic mirror at the back wall of the thruster, which reduces plasma losses to this surface, and a magnetic nozzle along the discharge channel, enhancing the ambipolar acceleration of the plasma which results in a quasineutral exhaust plume – eliminating the need for an external neutralizer. Plasma losses to the chamber walls are further reduced as the axial field lines restrict the motion of the electrons.[6]

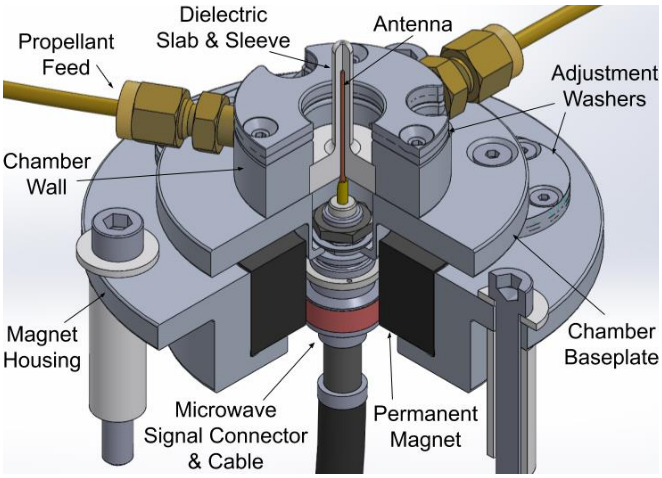

a)

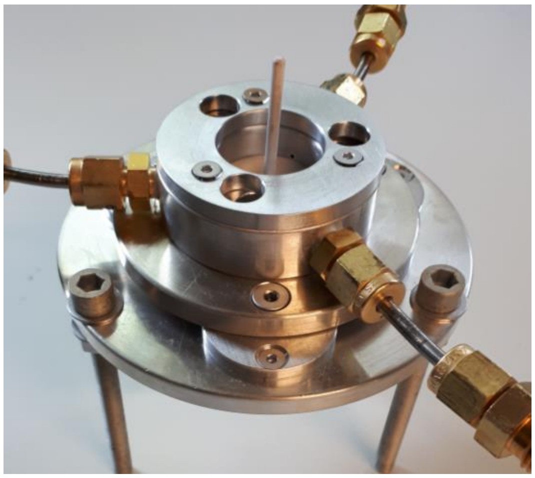

b)

Figure 1. a) Cutaway view of the AQUAJET thruster 3D model, highlighting the main thruster components. b) Photograph of the AQUAJET thruster assembly.

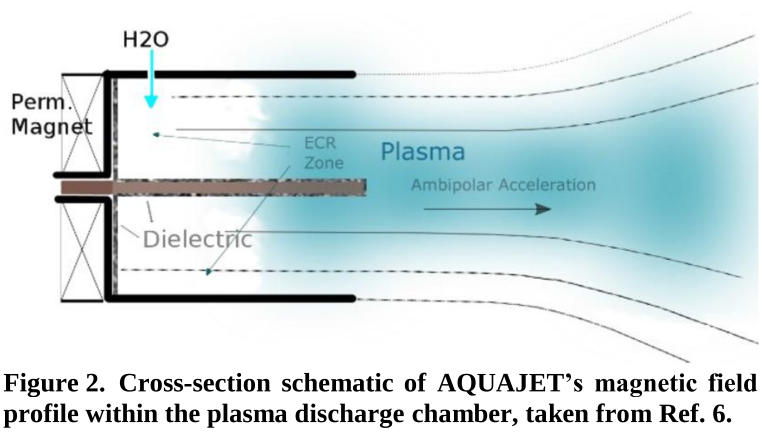

Figure 2. Cross-section schematic of AQUAJET's magnetic field profile within the plasma discharge chamber, taken from Ref. 6.

The ECR heating mechanism, induced by the application of a microwave frequency to a suitable magnetic field, allows for significantly higher electron temperatures to be achieved compared to those attainable with RF discharge sources[7]. For a microwave source frequency of 2.45 GHz, a magnetic field strength of 875 Gauss is required to satisfy the conditions necessary to achieving an ECR effect. A simulation of the magnetic field, given in Fig. 3, shows the location of the ECR zone close to the back wall of the chamber. Neutral propellant is injected into the discharge chamber near the back wall of the thruster and becomes ionized by ECR heating within the resonance zone, creating a high-density plasma in this region. Electrons in the discharge chamber are radially confined by the magnetic force due to the applied magnetic field, causing them to gyrate along the field lines. The collection of gyrating electrons produces an azimuthal plasma electric field, thus generating a plasma-induced magnetic field in opposition to the applied magnetic field. The two opposing magnetic fields repel each other, causing the hot electrons to expand and travel downstream of the thruster and cool down, generating an ambipolar electric field. The ambipolar field causes the ions to expand radially and accelerates them in the axial direction, as the thermal energy from the electrons converts into kinetic ion energy. As the field lines in the magnetic nozzle diverge downstream of the thruster, the plasma density decreases both radially and axially, allowing the high-velocity ions and hot, energetic electrons in the plasma to become demagnetized and detach from the magnetic field lines, resulting in a net thrust force. [6]

As the AQUAJET thruster is gridless and cathodeless, it is expected to provide a longer lifetime, greater reliability, and a significant reduction in the cost and complexity of the propulsion system compared to mature technologies currently in use[8]. Additionally, the elimination of the neutralizer allows for compatibility of the thruster with a wide range of atomic and molecular propellants, such as CO_2, H_2O and O_2[9,6].

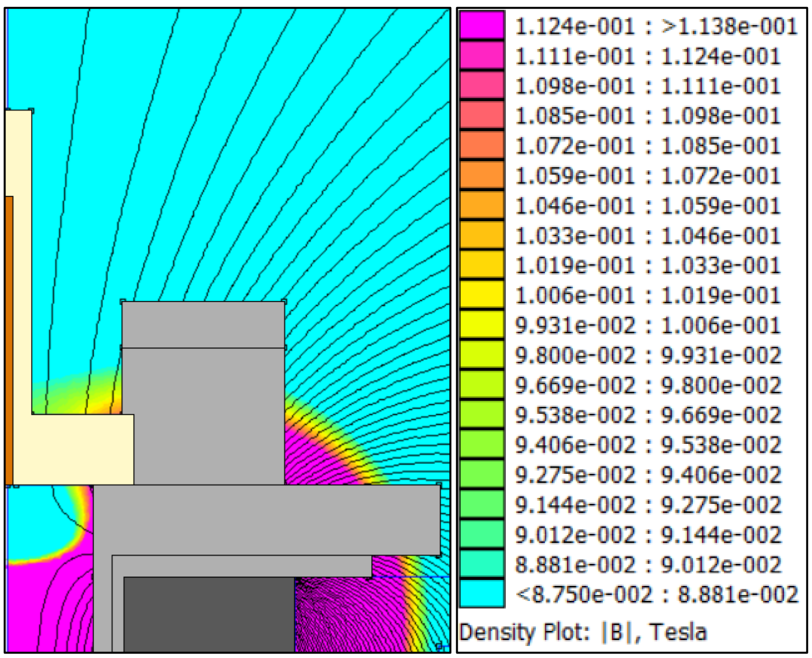

Figure 3. Simulation of AQUAJET's magnetic field profile, highlighting the ECR zone (0.0875-0.1138 T). Image shows the antenna (orange), dielectric sleeve and slab (beige), discharge chamber and thruster housing (light grey), and magnet (dark grey).

III.Experimental Setup for Thruster Validation and Performance Measurements

Experimental validation and performance measurements of the AQUAJET thruster were carried out at the Electric Propulsion Laboratory at SSC, using two of the available vacuum facilities: Icarus, for the proof-of-concept validation testing, and Daedalus, for the performance measurements. AQUAJET was operated with a Kuhne electronic Microwave Components KU SG 2.45-250 A signal generator. The microwave signal line consisted of HUBER+SUHNER 7/16 SUCOFEED 1/2 HF FR, and Pasternak TNC RG142 coaxial cables, with a Radio Frequency Systems DC-BLOCK-4-7MF in series. Direct thrust measurements were obtained using a pendulum-type thrust balance.

A. Icarus Vacuum Test Facility

The Icarus vacuum test facility is one of the smaller test facilities available at SSC. It was chosen for its small volume, and simple pumping system, which allows for quick, and flexible experimental turnover that is particularly suited to successive testing of multiple thruster configurations. Icarus is compact, with internal dimensions of 30 cm x 30 cm x 60 cm; its pumping system employs a turbomolecular pump that can achieve a typical base pressure of approx. 10^{-6} Torr, and background pressure of approx. 10^{-5} Torr during thruster operation. The chamber is equipped with several feedthroughs for thruster power lines, propellant feedlines, various electrical connections, and sensors, and a viewing port for observing the thruster plume during operation.

B. Daedalus Vacuum Test Facility

Daedalus is the largest vacuum test facility available at SSC; it provides a high vacuum environment suitable for measuring thruster performance, and a large volume that allows for full expansion of the thruster plume. The Daedalus vacuum chamber measures 1.5 m in diameter and 3 m in length, with a two-stage pumping system incorporating a cryogenic pump in parallel with a turbomolecular pump to produce an overall pumping capacity of over 12,000 l/s (nominal for air), capable of achieving base pressures in the range of 10^{-6} Torr. The chamber is equipped with a variety of feedthroughs for propellant feedlines, thruster power lines, and various sensor signal lines, and a series of viewing ports at different locations around the chamber. Multiple pressure gauges are installed at critical locations along the vacuum system to measure pressure levels of the chamber and pumping lines. The experimental setup of AQUAJET on the thrust balance inside the Daedalus vacuum chamber is shown in Fig. 4.

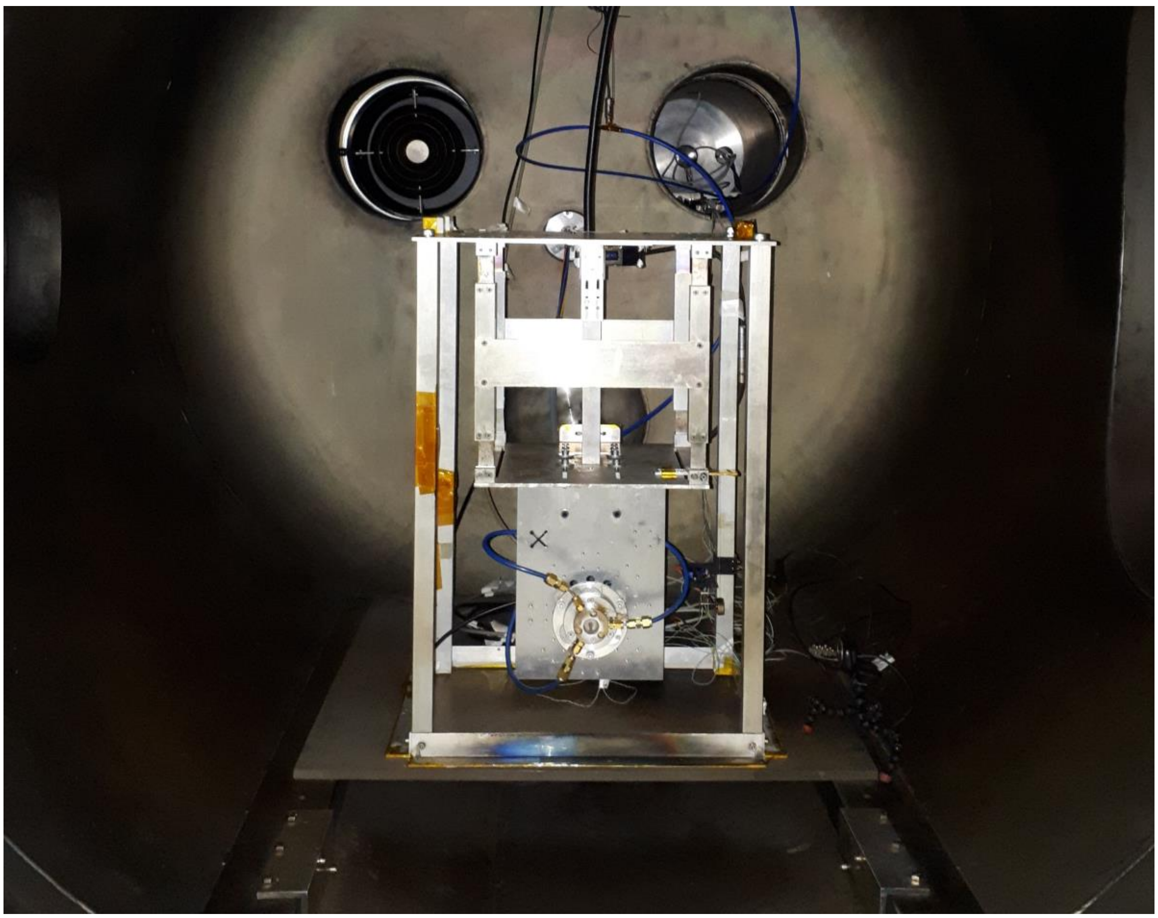

Figure 4. Experimental setup of AQUAJET in the Daedalus vacuum chamber. The thruster is mounted onto the thrust balance pendulum platform via an interface plate. Propellant feed lines (blue tubing), and microwave signal line (thick black cable) are visible in the image. The DC block is affixed to the back of the pendulum platform.

C. Thrust Balance

The performance measurements were obtained using a pendulum-type thrust balance. A full description of the thrust balance was previously published in Ref. 10 and 11. The thrust balance consists of a rigid frame supporting a moveable platform assembly which is attached by thin metal flexures allowing it to move back and forth in pendulum motion. A Micro-Epsilon model ILD 1700-2 laser sensor is mounted to the underside of the rigid support structure's top plate. The laser has a linearity of ± 0.1 % full scale output, and a resolution of 0.1µm. A laser target is mounted on top of the moveable platform, aligned with the laser sensor, to detect displacement of the platform. The thruster is mounted onto an interface plate attached to the moveable platform assembly. While the thruster is operating, the pendulum and, thus, the laser target become displaced from the zero position. This displacement is measured by the laser sensor and recorded by the ILD 1700 software.

There is inherent stiffness to the pendulum assembly that is increased by the addition of thruster cables, and propellant feedlines. To account for this, an automated calibration is performed using a rotational stage and pulley system to apply a range of calibration forces to the thrust balance, by moving a calibration mass**.** Calibration measurements of the final test setup are performed multiple times throughout the test campaign, under both hot, and cold conditions. The pendulum displacement data for the calibration is processed using MATLAB code. The code applies 5th order Butterworth filtering to the raw output signal data with a cut-off frequency of 0.5 Hz. The calibration coefficient is computed using linear regression of the force values applied to the platform versus the displacement values, as measured by the laser sensor. The uncertainty of the resulting calibration coefficient, which originates from the uncertainties of the mass value and geometrical dimensions, is computed using a Monte Carlo simulation algorithm that incorporates a large number of trials. The variables used in the simulation for the measurement and calibration processes consist of randomly generated values from within their individual probability distribution functions. Typical percentage uncertainties fall within a range of up to 15 %.

During thruster operation, thermal effects may cause a drift in the thrust measurements. In order to reduce the influence of thermal drift, the thrust data is obtained by switching off the thruster after stable operation is achieved, during the data acquisition process, thus producing a step change in the pendulum displacement. The thruster displacement data is processed using Python code to calculate the thrust value. Similar filtering is applied to the displacement step data. The displacement step change caused by the thruster switching off is automatically detected using a maximum derivative algorithm. Linear regression is applied to the data recorded before and after the thruster was switched off. (An example of a typical thrust step with post-processing and linear fit is given in Fig. 5.) The thrust value is then calculated from the displacement step, accounting for the calibration coefficient.

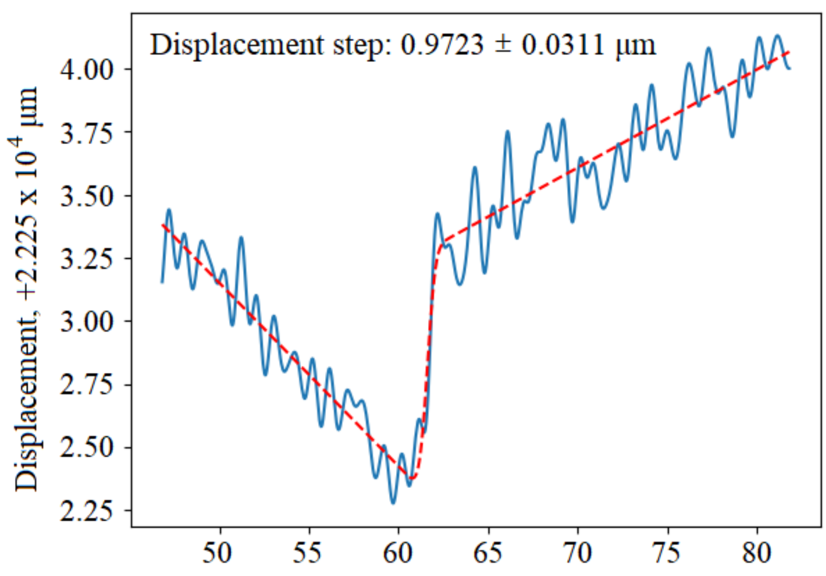

Figure 5. Typical thrust step measured by the laser displacement sensor, with post-processing filtering and maximum derivative algorithm applied. The linear fit for the thrust step is shown in red. Displacement step and uncertainty values are displayed.

D. Optical Emission Spectrometer

An Ocean Optics HR4000CG-UV-NIR spectrometer, with a wavelength range of 200-1100 nm, was used to measure the optical emission spectra of the plasma plume over time, to gain an understanding of the plasma properties of the thruster. The relative intensity of the peaks within the spectra provides insight into the ionization efficiency of the thruster under various operating conditions. According to the collisional radiative model (CRM) developed by Dressler et al.[12], the ratio of the 823 nm and 828 nm emission line intensities in xenon can be used to estimate the electron temperature of the plasma plume. According to a theoretical ambipolar acceleration mechanism, the specific impulse (i.e. ion velocity) is proportional to the square root of the electron temperature: $I_{sp} \propto \sqrt{T_e}$. An Ocean Optics 84-UV-25 long-distance collimating lens, with focal length of 100 mm, was focused on the central axis of the thruster exit plane to record the spectra of light being emitted by the thruster exhaust plume using OceanVIEW software.

IV.Results

The AQUAJET thruster was successfully operated with both noble gases (argon and xenon) and molecular propellant (water vapor) under a range of operating conditions and geometric configurations. Proof-of-concept validation testing was performed across the full operating envelope, with over 500 data points collected. Thruster operation was characterized to identify suitable thruster configurations for preliminary performance testing. Over 300 direct thrust measurements were collected while operating the thruster with argon, xenon, and water, over a range of power levels from 17-171 W, corresponding to thruster efficiencies in the range of 0.1-2.5 %. AQUAJET's thrust capabilities lie within the sub-milli-Newton range, leading to high levels of uncertainty in the thrust measurements as the thrust balance uncertainties increase in the <1mN regime. A number of optical emission spectra were recorded during thruster operation.

This section presents an overview of a reduced set of the data collected during the validation and performance characterization of the AQUAJET thruster. Floating potential of the thruster was measured at the discharge chamber assembly using a voltmeter. All operating power levels noted throughout the paper refer to the load power, which is typically measured as: forward power – reflected power. A short-hand naming convention for thruster configurations is used in this paper as follows: R = discharge chamber radius, in mm, L = discharge chamber length, in mm, and W = the thickness, in mm, of a spacer washer placed between the magnet and discharge chamber to adjust the ECR zone position.

A. Thruster Validation

Proof-of-concept validation testing of the AQUAJET thruster in the small Icarus chamber was successfully demonstrated over the full operating envelope, while keeping the ECR zone position fixed, and the microwave frequency constant at 2.45 GHz. Stable operations and reliable thruster ignitions were observed across all geometric configurations tested for the majority of operating conditions used. The thruster was operated at power levels in the range of 15-120 W for 3-4 mass flow rates of both argon, and water, with no obvious instances of erosion. Argon was tested with measured and controlled mass flow rates of 0.1, 0.2, and 0.3 mg/s, whereas water was tested with 4 different, yet arbitrary, mass flow rates (A < B < C < D) based on initial chamber pressures using a manual flow valve. Fig. 6 shows the AQUAJET thruster operating with a) argon, and b) water. Some plasma instabilities were observed at higher power levels with the 12 mm radius chamber, and at lower mass flow rates for some configurations accounting for < 10 % of the thruster tests; however, this may be corrected in future testing with the addition of a load matching network in line with the microwave signal.

Specific trends between thruster geometry, and operating conditions were difficult to define due to the compact volume of the vacuum chamber which leads to entrainment mass flow, resulting in increased chamber pressure, and reduced floating potential. However, for the majority of configurations, the percentage of reflected power consistently increased with input power, ranging between 0.1-30 %, overall – a sample of the data is shown in Fig. 7. These figures demonstrated that the primary variables affecting reflected power percentage are the chamber radius, and length, with mass flow rate causing only minor differences. Shorter lengths, and larger radii clearly minimized the reflected power, confirming the design expectations, as the AQUAJET thruster was designed for optimized impedance matching at the shortest chamber lengths.

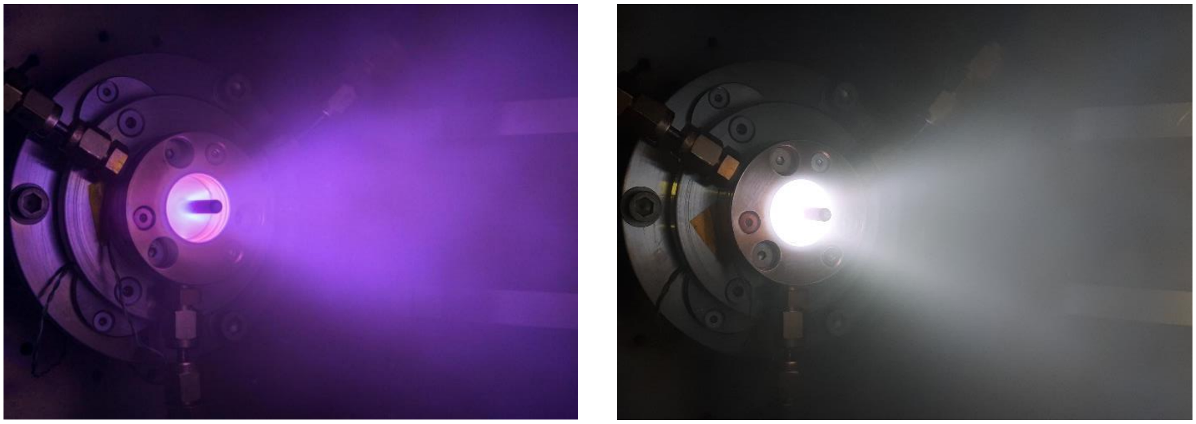

a) Argon b) Water

Figure 6. The AQUAJET thruster operating with a) argon, and b) water.

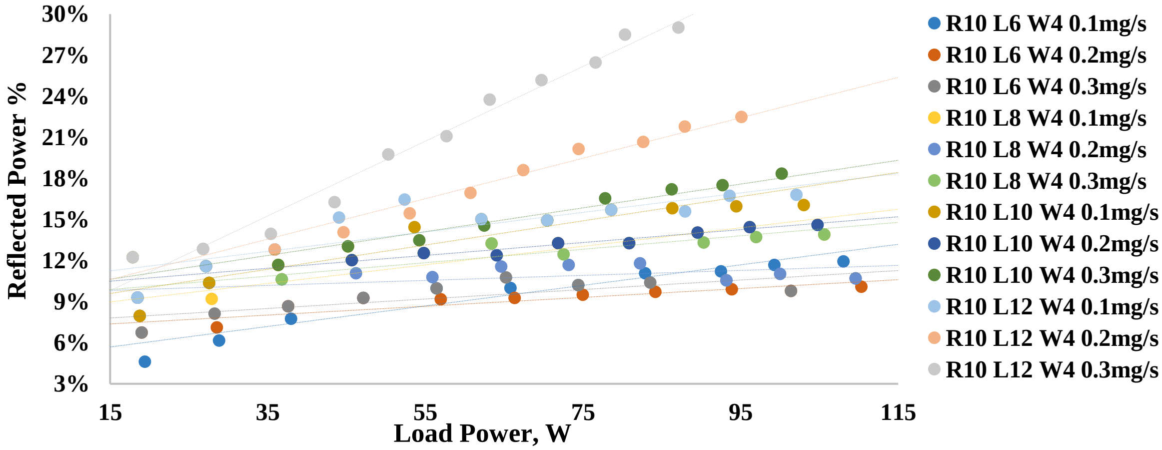

Figure 7. Sample validation data for AQUAJET operating with argon at 0.1, 0.2, and 0.3 mg/s, showing reflected power % as a function of load power for the R10 W4 thruster configuration with a range of chamber lengths: L6, L8, L10, and L12.

B. Thruster Performance

Performance measurements of AQUAJET were obtained in the larger chamber, Daedalus, while operating the thruster with noble gases (argon, and xenon), and molecular propellant (water vapor) under a selection of geometric configurations. Measurements were taken at power levels in the range of 17-171 W, for 2-3 mass flow rates: 0.1, and 0.2 mg/s for argon, 0.05, 0.1, and 0.2 mg/s for xenon, and 0.14, and 0.4 mg/s for water. The preliminary results show a roughly linear increase in the thrust, and specific impulse with power, confirming the scalability of this technology to higher power, with a promising rate of up to 5 s of specific impulse per Watt of input power.

Figure 8 shows a comparison of the thruster plume while operating with a) xenon, and b) water at 90 W. Visual observation of the images in Fig. 8 suggests that a higher plume divergence, and lower propellant utilization efficiency can be expected from water in comparison to xenon. This effect will be rigorously verified in future experiments via spatially-resolved ion current measurement using a Faraday probe mounted on a rotating arm.

To provide an overview of the complete set of performance measurements, the general trends for the average thrust, reflected power, and floating potential, with respect to the forward power are given in Fig. 9. The error bars contained within the graph correspond to the standard deviation of the measurements taken for each geometric configuration, and operating condition, with a minimum of three repetitions recorded for each data point. Each of the trends show a linear increase with forward power, as expected. The steeper incline of the floating potential compared to thrust is consistent with their relationships to electron temperature: the floating potential is proportional to the electron temperature, whereas thrust is proportional to its square root.

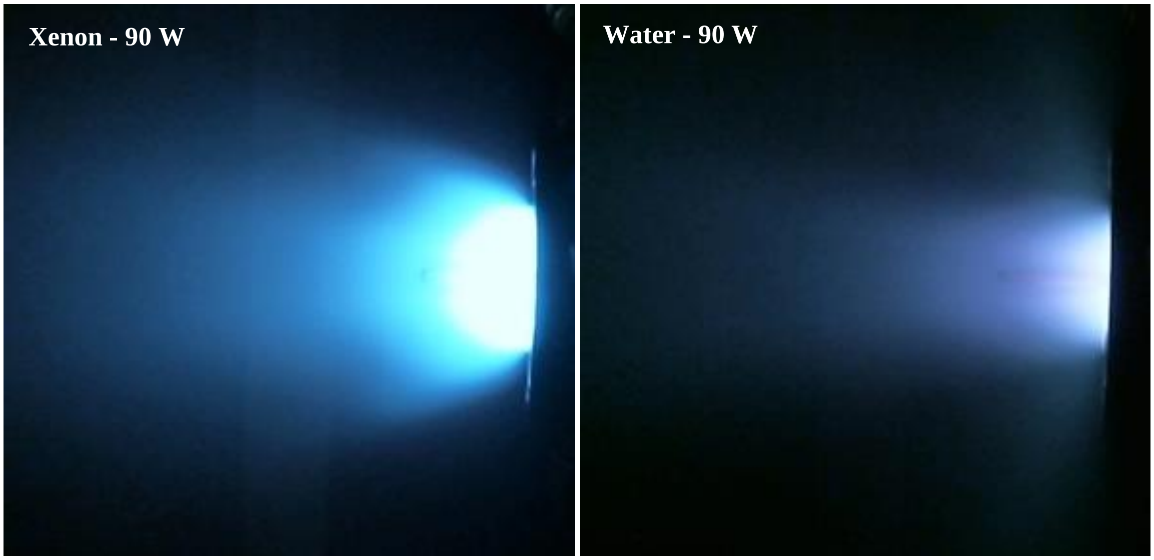

a) Xenon - 90 W b) Water - 90 W

Figure 8. Photographs of the AQUAJET thruster exhaust plume while operating at 90 W with a) xenon, and b) water. (These images do not reflect the true color of the plasma as they were captured with a desktop webcam that was not designed for use in vacuum.)

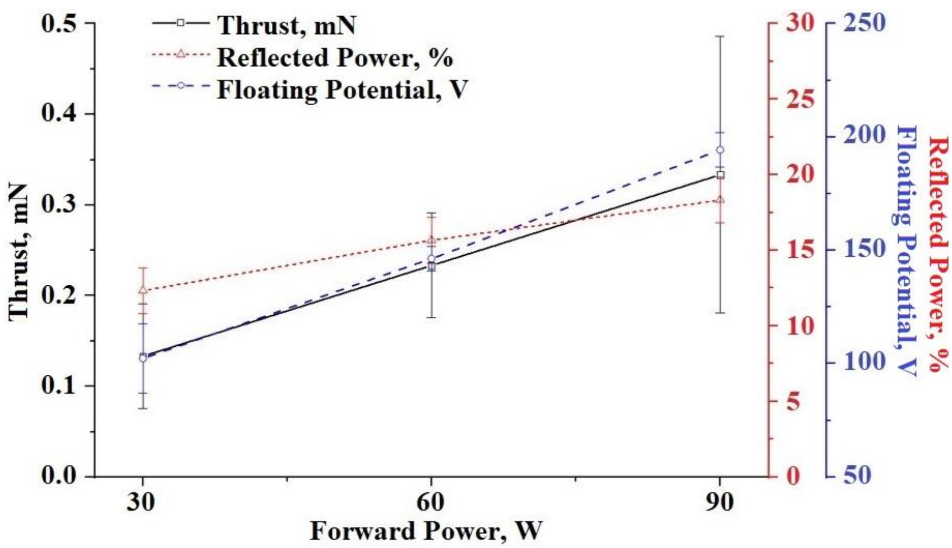

Figure 9. Representative trends in the results data for thruster configuration: R10 L12 W4, operating with xenon.

Figures 10, and 11 provide a sample of the performance measurements to demonstrate how the choice of propellant, thruster geometry, and mass flow rate affect the performance. a) Thrust, b) specific impulse, and c) thruster efficiency are plotted against load power in both figures, with Fig. 10 covering two different thruster configurations (radius 10 mm, length 10 mm, and radius 12 mm, length 12mm), both with a 2 mm magnet spacer washer and operating at 2.45 GHz, with xenon at two mass flow rates of 0.1 mg/s, and 0.2 mg/s. Figure 11 shows a single thruster configuration of radius 12 mm, length 12 mm, with a 2 mm magnet spacer washer operating at 2.45 GHz, with each of the three propellants under a range of mass flow rates: 0.1 mg/s, and 0.2 mg/s for argon, 0.05 mg/s, 0.1 mg/s, and 0.2 mg/s for xenon, and 0.4 mg/s for water. It was necessary to use a higher mass flow rate for the majority of the water performance measurements, as the thruster operation was not consistently stable with lower water flow rates; as a result, reduced ionization fraction and performance metrics are expected.

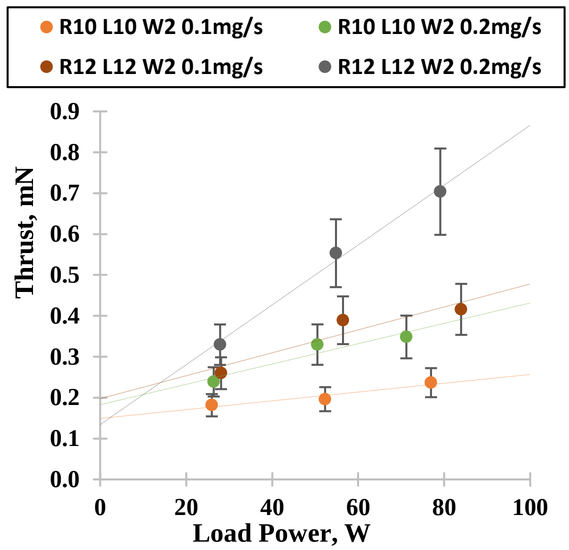

a) Thrust against load power.

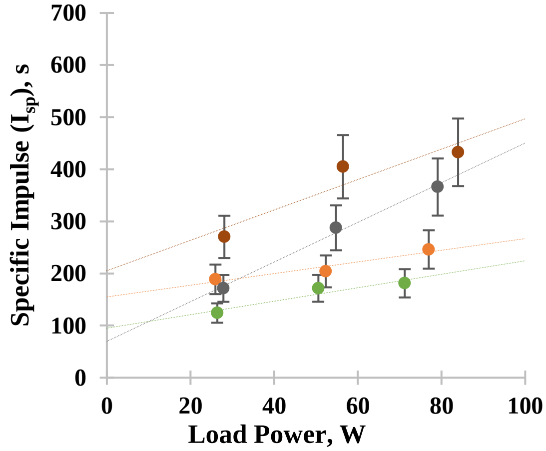

b) Specific impulse against load power.

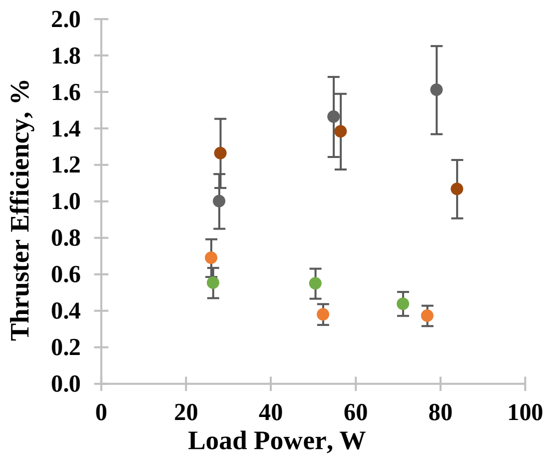

c) Thruster efficiency against load power.

Figure 10. Performance comparison of R10 L10 W2, and R12 L12 W2, operating at 2.45 GHz with

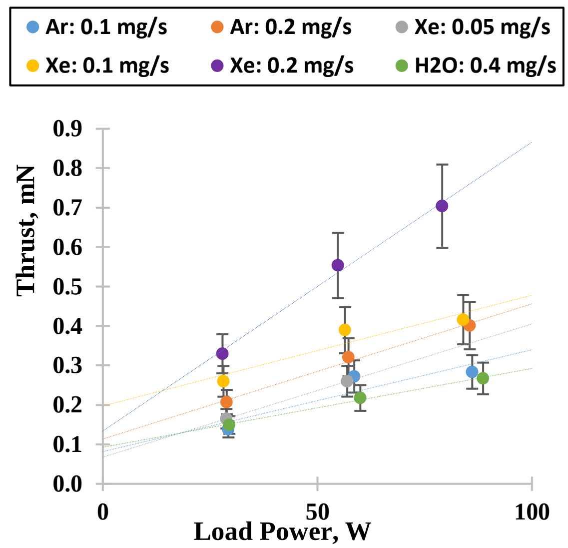

a) Thrust against load power.

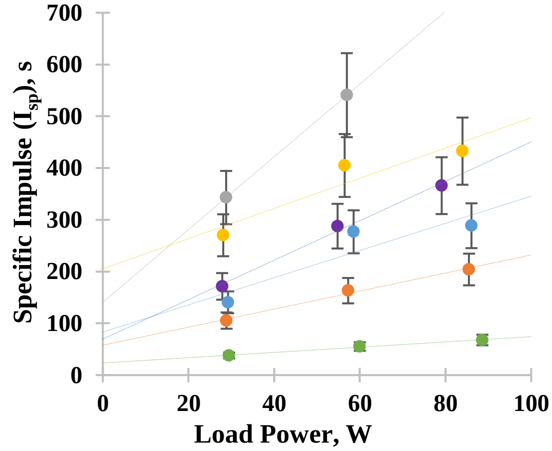

b) Specific impulse against load power.

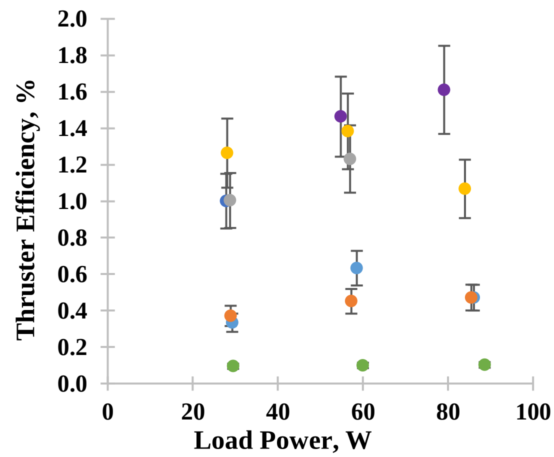

c) Thruster efficiency against load power.

Figure 11. Performance comparison of R12 L12 W2 operating at 2.45 GHz with Ar, Xe, and H_2O.

An overall improvement in all performance metrics is observed with increased thruster radius and length. Both the thrust, and specific impulse increase almost linearly with load power, confirming the scalability of the AQUAJET thruster technology. Each thruster configuration shows increased thrust, and reduced specific impulse, with increased mass flow rate, consistent with the relationship: $T = I_{sp}\dot{m}_p g_0$. Xenon is the proven propellant choice for electric propulsion, due to its high atomic mass, and low ionization potential, leading to high performance metrics. Argon is a potential contender with xenon; however, it has a lower atomic mass, and higher ionization potential, resulting in reduced performance capabilities. In comparison with the noble gases, water vapor has a similar ionization potential, significantly lower atomic mass, and is prone to power losses typical of molecular propellants (vibrational modes, molecular dissociation, etc.) which would lead to a notable reduction in performance; however, for certain missions, this disadvantage may be outweighed by the benefits of operating the thruster with a low-cost, easily accessible, "green" propellant. The results presented in Fig. 11 are consistent with this relationship.

As mentioned earlier, the power levels noted throughout the paper refer to the load power, taken as the forward power – reflected power; however, this does not take into account the power losses within the microwave lines. When taking estimated microwave line losses, and their uncertainties into account, the actual power delivered to the plasma (i.e. the absorbed power) may have ranged between 10-120 W, which would correspond to efficiencies of 0.1-8.2 %. Further work on experimentally quantifying the microwave line losses is required; however, these losses will be significantly reduced in future testing through a simplified microwave line design.

Table 1. Performance comparison of AQUAJET and Onera ECR thrusters.[13]

Thruster	Gas	$\dot{m}_p$, mg/s	P, W	T, mN	I_{sp}, s	η_T, %	P_{bg}, mbar
Onera ECR - ø 27 mm:	Xe	0.1	30	0.98	993	16	6×10^{-6} - 2×10^{-5}
	Xe	0.2	30	0.97	495	8	6×10^{-6} - 2×10^{-5}
	Xe	0.4	30	0.825	210	3	6×10^{-6} - 2×10^{-5}
AQUAJET - ø 24 mm:	Xe	0.10	28	0.3	270	1.3	6.7×10^{-6}
	Xe	0.20	28	0.3	171	1.0	1.1×10^{-5}
	H_2O	0.40	29	0.1	38	0.1	3.1×10^{-5}
Onera ECR - ø 13 mm:	Ar	0.1	35.7	0.3	315	1.3	6×10^{-6} - 2×10^{-5}
	Ar	0.2	37.3	0.5	257	1.7	6×10^{-6} - 2×10^{-5}
	Xe	0.1	40.4	0.6	590	4.2	6×10^{-6} - 2×10^{-5}
	Xe	0.2	40.7	0.8	428	4.3	6×10^{-6} - 2×10^{-5}
AQUAJET - ø 20 mm:	Ar	0.10	26 - 52	0.2 - 0.3	186 - 332	0.6 - 1.0	2.9×10^{-5}
	Ar	0.20	26 - 51	0.2 - 0.3	92 - 164	0.3 - 0.5	4.5×10^{-5}
AQUAJET - ø 16 mm:	Xe	0.10	49	0.3	319	1.0	9.7×10^{-6}
	Xe	0.20	40	0.4	198	0.9	2.5×10^{-5}
	H_2O	0.14	28 - 56	0.1 - 0.2	53 - 126	0.1 - 0.2	3.3×10^{-5}

The AQUAJET ECR thruster project was inspired by the promising results demonstrated by Cannat, et al.[13] with the Onera ECR thruster. This technology provides a suitable comparison for the AQUAJET performance metrics, as both thrusters hold similar geometric configurations, and operate within the same operating conditions. Table 1 shows a comparison of the AQUAJET performance metrics against those presented by Cannat, et al.[13] for similar thruster configurations, and operating conditions for argon (Ar), and xenon (Xe). The AQUAJET performance metrics for water (H_2O) have also been included. The performance metrics presented in the table include the indirect estimations, taken from plasma probe measurements, on the Onera ECR thruster (as presented in Ref. 13), and the direct thruster measurements recorded with AQUAJET. A study of the effects of background pressure on the performance of the Onera ECR thruster, presented by Vialis, et al.[14], has demonstrated that performance measurements are highly sensitive to the background pressure. It is suggested that a significant improvement in performance levels might be observed for lower background pressure. An average increase of ~3.5×10^{-6} Torr was found between xenon and argon for the same mass flow rates during the AQUAJET performance testing. As such, the lower performance metrics for AQUAJET, outlined in the comparison with Onera, may be influenced by the background pressure effects.

C. Optical Emission Spectra

A sample of the optical emission spectra obtained for a xenon plasma plume, during thruster operation, are presented in Fig. 12, showing a comparison of the spectra at different power levels: a) 60 W, and b) 90 W. The spectra shown below were measured with the same thruster configuration (radius 12 mm, length 12 mm, with a 2 mm magnet spacer washer), and operating conditions (2.45 GHz with a mass flow rate of 0.2 mg/s). The main xenon emission lines are clearly visible in the spectra. The intensity ratio of the 823 nm, and 828 nm emission lines (I823/I828) gives a value of 2.3, suggesting electron temperatures of less than 5 eV (based on the collisional radiative model presented by Dressler et al.[12]). The low electron temperature is indicative of the lower performance metrics observed in comparison to the Onera ECR thruster, where electron temperatures of over 10 eV were achieved for 20 W absorbed power[13]. As the power is increased from 60 W to 90 W, a reduction in the intensity of the 895-904 nm cluster, and an increase in the intensity of the 461-543 nm cluster is observed. This signifies an increase in the propellant ionization fraction, consistent with an increase in electron temperature, as the 895-904 nm cluster is populated by the neutral xenon atoms, Xe I, whereas the 461-543 nm cluster represents the singly ionized xenon atoms, Xe II.

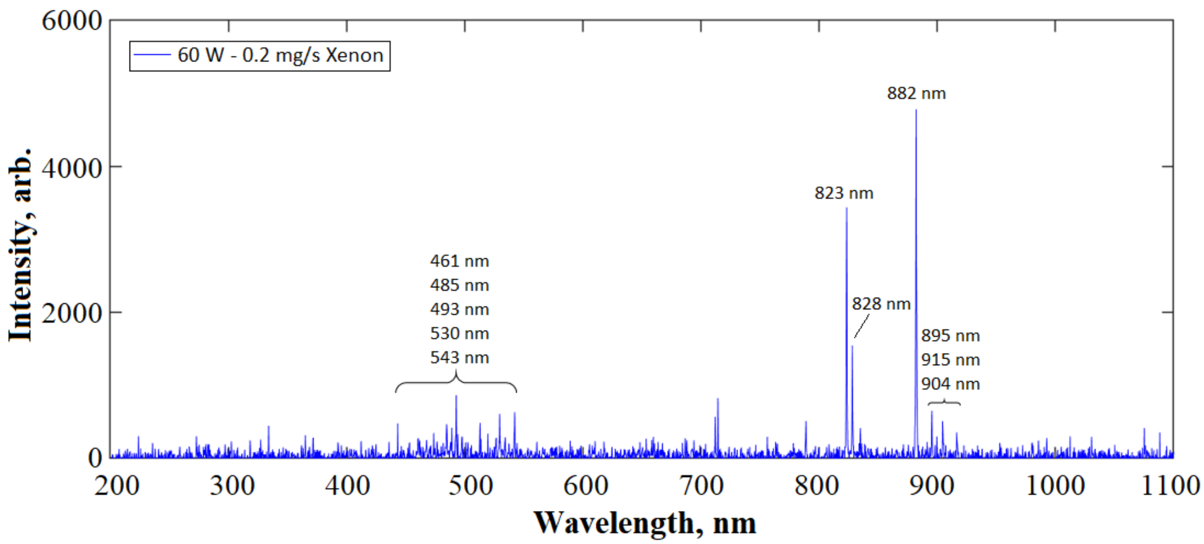

a) Xenon – 60 W

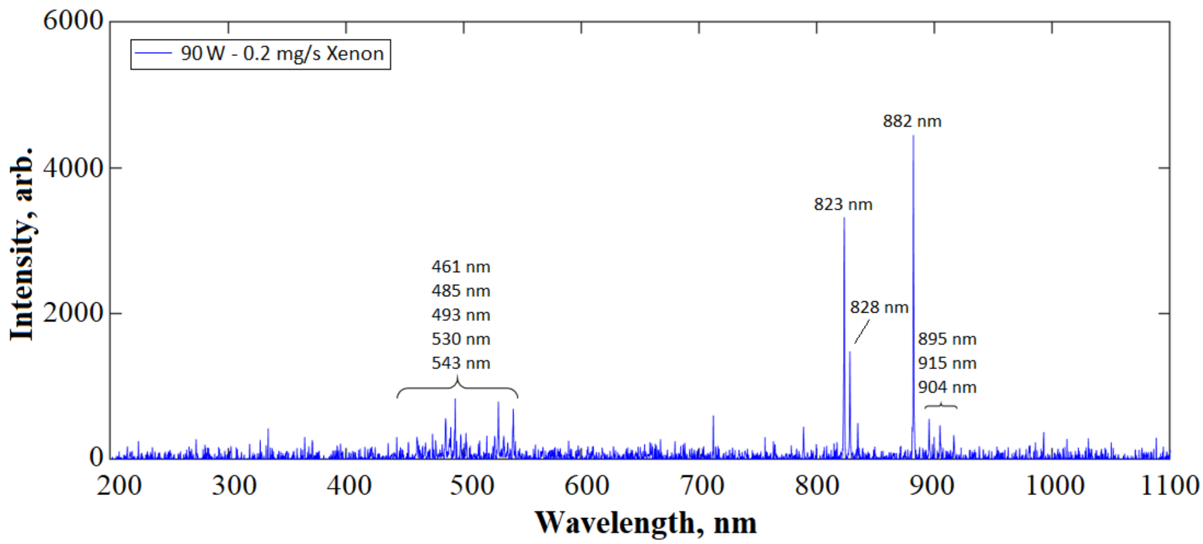

b) Xenon – 90 W

Figure 12. Optical emission spectra for the R12 L12 W2 AQUAJET thruster operating at 2.45 GHz with 0.2 mg/s of xenon at a) 60 W, and b) 90 W.

V.Conclusion

Successful proof-of-concept for the ECR thruster, operating with both noble gases, and molecular propellants has been demonstrated. The thruster has proven capable of operating at low-power levels, and mass flow rates suitable for applications with small satellites, as well as achieving stable operation at higher load power levels of up to 171 W. Preliminary testing has shown notably lower performance metrics against the most comparable thruster in literature; however, significant re-design and improvements of the thruster and microwave line are underway for the next model (as described by Rosati Azevedo, et al. in Ref. 15). In addition, upgrades to the SSC's Daedalus vacuum chamber pumping system are underway to improve the pumping capacity, and lower background pressure levels. In combination, it is hoped that this will allow for stable operation of the AQUAJET thruster with water at lower mass flow rates, to fully characterize its performance envelope. Additional testing of the thruster under improved vacuum conditions with a higher precision thrust balance (later this year) will fully quantify the AQUAJET thruster performance. The work performed to-date, and described in this paper, have demonstrated successful progress of the AQUAJET thruster development to TRL 4. The results and knowledge gained will aid in the development of a Scaled Engineering Model to demonstrate successful validation of the prototype components in a relevant environment, to achieve TRL 5.

Acknowledgments

The work described in this paper is funded by the UK Space Agency's National Space Technology Programme in the framework of the "NSTP3-FT-63" project. R. Moloney thanks the Institute of Mechanical Engineers for funding their attendance at the IEPC conference.

References

[1]Goebel, D. M., and Katz, I., *Fundamentals of Electric Propulsion: Ion and Hall Thrusters*, John Wiley & Sons, 2008.

[2]Oleson, S. R., and Sankovic, J. M., "Electric Propulsion for Low Earth Orbit Constellations," *Proceedings of JANNAF Propulsion Meeting*, Cleveland, Ohio, 1998.

[3]Wright, E., Taylor, G., and Tsitsilonis, N., "Small Satellite Market Intelligence: Q1 2019," *Satellite Applications Catapult Small Satellite Market Intelligence Report*, [online report], No. 8, URL: https://s3-eu-west-1.amazonaws.com/media.newsa.catapult/wp-content/uploads/2019/05/30124810/19052056-Small-Sat-Market-Intelligence-report-Q1-2019.pdf [cited 11 September 2019].

[4]Zhurindag, V. V., Kaufmanddag, H. R., and Robinson, R. S., "Physics of Closed Drift Thrusters," *Plasma Sources Science and Technology*, Vol. 8, No. 1, pp. R1–R20, 1999.

[5]Raitses, Y., and Fisch, N. J., "Parametric Investigations of a Nonconventional Hall Thruster," *Physics of Plasmas*, Vol. 8, No. 5, pp. 2579-2586, May 2001.

[6]D. Staab, et al., "AQUAJET: An Electrodeless ECR Water Thruster," *Proceedings of Space Propulsion Conference*, CP00359, Seville, Spain, 2018.

[7]Packan, D., et al., "The "MINOTOR" H2020 Project for ECR Thruster Development," *Proceedings of the 35th International Electric Propulsion Conference*, CP547, Atlanta, Georgia, 2017.

[8]Rafalskyi, D., and Aanesland, A., "Brief Review on Plasma Propulsion with Neutralizer-Free Systems," *Plasma Sources Science and Technology*, Vol. 25, No. 4, 18 May 2016.

[9]Charles, C., Boswell, R. W., Laine, R., and MacLellan, P., "An Experimental Investigation of Alternative Propellants for the Helicon Double Layer Thruster," *Journal of Physics D: Applied Physics*, Vol. 41, No. 17, 21 Aug. 2008.

[10]Lucca Fabris, A., et al., "An Interlaboratory Comparison of Thrust Measurements for a 200W Quad Confinement Thruster," *Proceedings of Space Propulsion Conference*, CP3124797, Rome, Italy, 2016.

[11]Lucca Fabris, A., et al., "Vacuum Facility Effects on Quad Confinement Thruster Testing," *Proceedings of the 35th International Electric Propulsion Conference*, CP250, Atlanta, Georgia, 2017.

[12]Dressler, R. A., et al., "Near-Infrared Collisional Radiative Model for Xe Plasma Electrostatic Thrusters: The Role of Metastable Atoms," *Journal of Physics D: Applied Physics*, Vol. 42, No. 18, 21 Sep. 2009.

[13]Cannat, F., et al., "Optimization of a Coaxial Electron Cyclotron Resonance Plasma Thruster with an Analytical Model," *Physics of Plasmas, American Institute of Physics*, Vol. 22, pp. 053503, 2015.

[14]Vialis, T., Jarrige, J., and Packan, D., "Geometry Optimization and Effect of Gas Propellant in an Electron Cyclotron Resonance Plasma Thruster," *Proceedings of the 35th International Electric Propulsion Conference*, CP378, Atlanta, Georgia, 2017.

[15]Rosati Azevedo, E., et al., "Analytical Plasma Modelling and Design Upgrade for an ECR Thruster Operating on Water and Ammonia Propellants," *Proceedings of the 36th International Electric Propulsion Conference*, CP638, Vienna, Austria, 2019, (to be published).